

DISCLAIMER

DEC 1 8 1985

This report was prepared as an account of work sponsored by an agency of the United States Government. Neither the United States Government nor any agency thereof, nor any of their employees, makes any warranty, express or implied, or assumes any legal liability or responsibility for the accuracy, completeness, or usefulness of any information, apparatus, product, or process disclosed, or represents that its use would not infringe privately owned rights. Reference herein to any specific commercial product, process, or service by trade name, trademark, manufacturer, or otherwise does not necessarily constitute or imply its endorsement, recommendation, or favoring by the United States Government or any agency thereof. The views and opinions of authors expressed herein do not necessarily state or reflect those of the United States Government or any agency thereof.

CORE DESIGN AND PERFORMANCE OF SMALL INHERENTLY SAFE LMRs

CONF-860302--1

Y. Orechwa, H. Khalil, R. B. Turski, and E. K. Fujita
Applied Physics Division
Argonne National Laboratory
Argonne, Illinois 60439
(312) 972-4876

DE86 004071

ABSTRACT

Oxide and metal-fueled core designs at the 900 Mwt level and constrained by a requirement for interchangeability are described. The physics parameters of the two cores studied here indicate that metal-fueled cores display attractive economic and safety features and are more flexible than are oxide cores in adapting to currently-changing deployment scenarios.

previous designs -- thereby reducing the cost of the reactor system.

In order to fully realize these economic and safety features of the LMR, a detailed analysis has been performed of cores designed to the reactor specifications shown in Table I.

TABLE I. General Reactor Specifications

Reactor Power, Mwt	900
Core Concept	Heterogeneous
Reactor Outlet Temperature, °C(°F)	510 (950)
Reactor ΔT, °C(°F)	135 (275)
Fuel Residence Time, Cycles	
Driver	4
Internal Blanket	4
Radial Blanket	4
Structural Material	HT-9
Cycle Length, days	365
Capacity Factor	80%

INTRODUCTION

The initially-projected demand for increasing nuclear generating capacity and the subsequent rise in the price of uranium have not materialized in the U.S. Consequently, the perception of an early need for LMFBRs has changed significantly. In addition, the previous assumption that the capital cost differential between a LWR and a LMFBR would be overcome through a lower fuel cycle cost as the price of uranium increased is, under current projections, no longer tenable, and the LMFBR must therefore penetrate the U.S. electricity generating market on its own merits, taking into account the pre-vailing political, social, and economic forces.

The 900 Mwt reactor output is consistent with currently-perceived deployment scenarios where the reactors are built sequentially, at one site, at a pace which matches the growth in the demand for electricity. This size may also allow factory fabrication of modular components and their subsequent transportation from factory to reactor site.

To meet these new conditions for LMFBR deployment, present efforts in core design focus on concepts which respond to current economic and social realities. For example, in the U.S., recent core design efforts have shifted from 1000 MWe and greater plant sizes to much smaller outputs of 300 MWe and below. This approach, it is felt, is appropriate in view of the slower growth rate in electricity demand and current financial constraints. In addition, current LMR core design activities have placed emphasis on the maximum enhancement of the inherent reactivity feedbacks and larger thermal inertia of the LMR pool design. It is felt that a demonstrable inherently safe LMR core design should contribute to making nuclear power more socially acceptable and should allow the removal of costly safety systems associated with

To fully evaluate the economic and inherent safety potential of LMRs, there are strong incentives for analyzing core designs with metal-based fuel in addition to oxide fuel. Metal fuel has not received widespread attention for large LMFBR application over the last two decades, primarily due to previously unfavorable high burnup fuel performance characteristics and

MASTER

jsw

a high mixed mean outlet temperature requirement. Recent developments, however, indicate that metal fuel performance comparable and perhaps even superior to that of oxide fuel can be achieved.² Further, calculations indicate that the high thermal conductivity of metal fuel enhances the inherent safety response of the system, especially during loss-of-flow-without-scrum transients.³ Metal fuel also allows for a compact, simplified integral fuel cycle with uranium startup.^{4,5}

The maximization of breeding is currently not perceived as the main goal of LMR design; however, it is still considered central, as it affects fuel management and design considerations such as control requirements and reactivity available for TOP initiation. In this context, the superior breeding of the metal-fueled cores has proven to provide for greater flexibility in adapting its fuel cycle and its management to changing external cycle requirements and deployment scenarios.

REACTOR CORE DESIGN

The core configuration was developed to meet the reactor performance specifications of Table I and the following constraints:

- an interchangeable layout for oxide and metal fueled assemblies
- a "self-regenerative" fissile breeding gain equal to the anticipated loss during reprocessing.

The resulting radially-heterogeneous core configuration is shown in Fig. 1. It consists of 102 driver assemblies, 85 blanket assemblies, 12 control assemblies, and 180 reflector assemblies. The approach to shielding in this layout is to use two types of reflector assemblies: 54 steel assemblies in the first row; and 126 assemblies containing B_4C in the last two rows.

The fuel assemblies were designed to take into account the above constraints. These are primarily reflected in the choice of HT-9 as the structural material, and of the fuel pin diameter, core height, and the sizing of the duct and interassembly sodium gap. A description of the fuel design parameters is given in Table II. The constraints of annual refueling and a discharge burnup limit of ~150 MWd/kg limit the choice of fuel pin diameter and result in the slight difference in the fuel pin diameter between metal and oxide fuel. However, the main differences in the assembly parameters with respect to fuel type arise from the difference in the fast fluence. The 35% higher fluence in the metal core ($3.42 \times 10^{23}n/cm^2$ to $2.54 \times 10^{23}n/cm^2$) dictates the need for a stronger duct (0.140 in. to 0.130 in.) and a

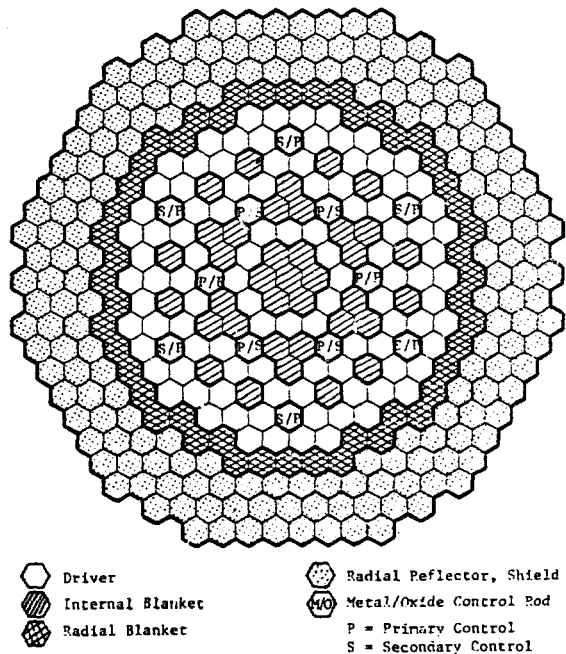


Fig. 1. Core Layout for Metal and Oxide Fuel

larger interassembly gap (0.150 in. to 0.100 in.) to accommodate the proportionate increase in irradiation induced creep and swelling. Due to the use of the low swelling ferritic alloy HT-9 in these cores, the duct dilation is due almost exclusively to pressure-driven irradiation induced creep. The interchangeability constraint can be met due to the slightly smaller fuel pin diameter in the metal core which allows for a thicker duct and a larger interassembly gap. The active fuel length of the metal-fueled core is 10% less than that of the oxide core, which is merely a reflection of the higher allowable linear power for metal fuel (in this case 10%).

A different blanket design approach was adopted between the two fuel types, based on tailoring the fissile breeding gain to a self-regenerative amount which just compensates for anticipated losses during reprocessing. For the oxide core, the necessary breeding was achieved by adjusting the axial blanket thickness; a six inch blanket above and below the core was found to satisfy the breeding requirement with some margin. For the metal core, the axial blanket was eliminated entirely to simplify the steps of the proposed pyrometallurgical process for fuel reprocessing. To compensate for the loss in breeding by elimination of the axial blanket in the metal core, the length of the internal and radial blankets was increased by 8 inches with respect to the fueled height of the driver assemblies.

TABLE II. Driver Assembly Design Parameters

	Metal	Oxide
Fuel Material	U-Pu-Zr	UO ₂ -PuO ₂
Cladding and Duct Material	HT-9	HT-9
Number of Pins per Assembly	271	271
Fuel Pin Diameter, cm (in.)	0.724 (0.285)	0.737 (0.290)
Cladding Thickness, cm (in.)	0.056 (0.022)	0.056 (0.022)
Pitch/Diameter Ratio	1.18	1.18
Fuel Smear Density, % T.D.	75	82.5
Active Fuel Length, cm (in.)	91.4 (36)	101.6 (40)
Axial Blanket Thickness, cm (in.)	-	15.24 (6)
Duct Outside Flat-to-Flat, cm (in.)	15.01 (5.911)	15.21 (5.990)
Duct Wall Thickness, cm (in.)	0.356 (0.140)	0.330 (0.130)
Interassembly Gap, cm (in.)	0.381 (0.150)	0.254 (0.100)
Assembly Lattice Pitch, cm (in.)	15.39 (6.061)	15.47 (6.090)

NEUTRONIC PERFORMANCE

The neutronic performance parameters for an equilibrium cycle are summarized in Table III for the metal and oxide designs. These parameters were calculated in hexagonal-Z geometry using eight neutron energy groups. The residence time is four cycles for both the driver and blanket assemblies. The fuel management assumes four batch annual refueling with scatter reloading. The Pu isotopes are those for a self-regenerative recycle mode at equilibrium.

The power fractions and power peaking factors given in Table III show little difference between the metal and oxide fueled cores. The peak linear powers of 40.2 kW/m (12.25 kW/ft) and 36.2 kW/m (11.05 kW/ft) for the metal and oxide cores respectively lie within the design limit of 49.2 kW/m (15.0 kW/ft) and 44.3 kW/m (13.5 kW/ft).

The higher heavy metal density of metal fuel coupled with its enhanced breeding characteristics allows for a slightly smaller pin size in the metal design while still satisfying self-regenerative breeding requirements. The breeding ratio for the metal core (with no axial blanket) is 1.023 and compared to the oxide core (with axial blanket) of 1.051, see Table IV.

Even though the metal design has a lower fuel volume fraction as the result of a smaller pin size and lower fuel smeared density (75% to 82.5%), the higher density of metal fuel results in a larger initial loading of heavy metal in the driver region (7883.8 kg to 6948.9 kg). The higher heavy metal loading in the metal core results in a lower fissile loading and corresponding lower enrichment (18.7% to 23.8%).

The higher fuel density and lower enrichment result in a higher conversion ratio in the driver region which in turn is the basis for the lower reactivity swing over a cycle; 1.16% Δk for the metal compared to 1.65% Δk for the oxide design. The metal core, which has a smaller burnup swing, has a smaller amount of reactivity vested in the rod bank or a single rod; hence, the magnitude of the single rod runaway TOP initiator, is smaller for the metal core.

CONTROL SYSTEMS

Control system requirements for the different cores were estimated. These requirements consist of components which compensate for core temperature changes, fuel depletion, potential reactivity faults (the ejection of a control rod from the critical position), and for reactivity uncertainties

TABLE III. Equilibrium-Cycle Performance Parameters

	Metal			Oxide			
	Driver	Internal Blanket	Radial Blanket	Driver	Internal Blanket	Radial Blanket	Axial Blanket
Power Fraction, %							
BOEC	81.63	11.90	4.88	80.31	11.95	5.19	1.66
EOEC	76.24	16.26	6.09	74.15	16.31	6.43	2.19
Peak Linear Power, kW/m (kW/ft)							
BOEC	40.2 (12.25)	24.7 (7.53)	13.4 (4.11)	36.2 (11.05)	32.4 (9.89)	18.4 (5.60)	4.0 (1.21)
EOEC	37.4 (11.41)	32.2 (9.83)	15.7 (4.78)	33.3 (10.16)	42.2 (12.85)	21.2 (6.47)	5.3 (1.63)
Power Peaking Factor							
BOEC	1.38	1.61	2.78	1.41	1.87	3.16	2.24
EOEC	1.38	1.54	2.59	1.40	1.75	2.95	2.29
Peak Flux, $10^{15} \text{ cm}^{-2} \text{ s}^{-1}$							
BOEC	5.10	5.03	3.48	4.38	4.37	3.12	2.05
EOEC	5.21	5.16	3.38	4.36	4.33	2.99	2.20
Peak Fast Flux, $10^{15} \text{ cm}^{-2} \text{ s}^{-1}$							
BOEC	3.42	3.25	1.66	2.54	2.41	1.17	0.82
EOEC	3.41	3.28	1.63	2.51	2.36	1.14	0.88
Peak Fast Fluence, 10^{23} cm^{-2}	3.45	3.29	1.66	2.55	2.41	1.17	0.86
Peak Discharge Burnup, MWD/kg	143.3	48.8	24.1	162.4	51.0	25.90	18.52

TABLE IV. Reactor Performance Characteristics

	Metal	Oxide
Reactivity Swing, Δk	1.16	1.65
Breeding Ratio		
Driver	0.460	0.390
Internal Blanket	0.348	0.357
Radial Blanket	0.216	0.225
Axial Blanket		0.078
Total	1.023	1.051
Initial Loading, kg		
Heavy Metal		
Driver	7883.8	6948.9
Internal Blanket	4556.3	4969.4
Radial Blanket	5910.9	2161.7
Axial Blanket	-	6446.7
Total	18351.1	20526.7
Fissile		
Driver	1472.2	1653.7
Internal Blanket	9.1	9.9
Radial Blanket	11.8	4.3
Axial Blanket	-	12.9
Total	1493.2	1680.8
Net Fissile Gain, kg/yr		
Driver	-100.5	-122.5
Internal Blanket	60.8	67.4
Radial Blanket	45.9	17.8
Axial Blanket	-	52.0
Total	6.2	14.7

existing in criticality prediction and fissile enrichment. The control requirements are summarized in Table V. The hot-to-cold component is based on an assumed operating temperature of 1500°K for the oxide fuel and 1000°K for the metal fuel. (This component consists of subcomponents arising from the Doppler effect, fuel axial contraction, core radial contraction, and coolant contraction.) Note that the hot-to-cold component is larger for the oxide core than for the metal core. This difference is a consequence of the larger Doppler coefficient and the higher operating temperature of the oxide fuel; the higher axial contraction coefficient of the metal fuel is offset largely by its lower operating temperature.

Control rod worths have been evaluated for the two cores. For the metal core, the six row-4 control assemblies were designated as primary rods, while the six row-7 control positions were designated secondary rods. For the oxide core, the primary control system consisted of eight assemblies (six from row 7 and two from row 4), and the secondary system consisted of the four remaining row-4 control positions. The worths of the primary and secondary control systems were determined at BOEC in hexagonal-Z geometry using diffusion theory and eight groups. Table VI shows, as a function of $B_{10}C$ enrichment, the total worth of each control system, and its minimum worth allowing for any single stuck rod failure. By comparing the maximum requirements to the minimum worths, it may be seen that both control systems of the oxide core satisfy their requirements using $B_{10}C$ enriched to 50% in B-10.

TABLE V. Estimate of Control System Requirements

	Metal		Oxide	
	Primary System, % Δk	Secondary System, % Δk	Primary System, % Δk	Secondary System, % Δk
Hot to Cold ^a	0.63	0.39	1.28	0.99
Reactivity Fault ^b / Shutdown Margin ^c	0.23/ 1.00	0.23 1.00	0.35/ 1.00	0.35/ 1.00
Reactivity Excess ^d	1.53	-	2.10	-
Criticality Uncertainty ^e	± 0.3	-	± 0.3	-
Fissile Tolerance ^f	± 0.3	-	± 0.3	-
Total Requirement	3.16 ± 0.42	1.39	4.38 ± 0.42	1.99
Maximum Requirement	3.58	1.39	4.80	1.99

^aDetermined from total reactivity increase associated with decrease in temperature from operating temperature (800°K for metal 1300°K for oxide) to refueling temperature (477°K) for primary system or to standby temperature (588°K) for secondary system.

^bBased on runout of row-4 control rod.

^cA shutdown margin of 1.0% Δk is used because it exceeds the rod-runout worths.

^dDetermined from $1.15 * (\text{burnup reactivity swing}) + 0.2\% \Delta k$.

^eAssumed equal to CRBR value.

^fBased on an uncertainty of 0.5% in batch fissile enrichments.

TABLE VI. Control Rod Worths at BOEC (% Δk)

	Metal		Oxide	
	Primary Rods	Secondary Rods	Primary Rods	Secondary Rods
A. Natural B ₄ C (19.8% B-10)				
Total Worth	3.98	3.35	5.04	2.42
Stuck Rod Worth	0.63	0.95	1.72	0.69
Minimum Worth	3.35	2.40	3.32	1.73
B. Enriched B ₄ C (50% B-10)				
Total Worth	5.73	5.13	7.30	3.33
Stuck Rod Worth	1.01	1.45	2.16	1.00
Minimum Worth	4.72	3.67	5.14	2.33

For the metal core, natural B₂C (19.8% B-10 enrichment) can be used for the secondary rods, while the primary system meets its requirements with a 50% enrichment by a substantial margin.

REACTIVITY COEFFICIENTS

Reactivity feedback coefficients were computed for the two cores at EOE using twenty energy groups and the results are displayed in Table VII. The first order perturbation approximation was used to calculate coolant void worths and fuel Doppler coefficients, while differences in eigenvalues were used to determine the radial and axial expansion coefficients. Table VII shows that, as expected, the metal core has a higher coolant void worth and a lower Doppler coefficient than does the oxide core. The metal core is also seen to have a slightly more negative radial expansion coefficient. The fuel axial expansion coefficients, which were determined assuming the fuel is not restrained by the cladding, are similar for the oxide and metal cores when measured in reactivity worth per unit length of expansion.

The reactivity coefficients presented in Table VII do not by themselves show that metal cores have larger safety margins than do oxide cores. Others,⁶ however, have shown that the reactivity coefficient of metallic-fueled cores provide greater inherent safety margins than do oxide fueled designs, due solely to their intrinsic thermal, mechanical, and neutronic properties.

DESIGN FLEXIBILITY

The fact that metal-fueled systems have superior breeding characteristics to oxide fueled systems provides them with greater flexibility in adapting to changing deployment scenarios. In some cases, changes to the performance requirements of the plant require major changes to the oxide core design but only minor adjustments in the metal design. The following example is given to elucidate this point.

There is potential economic incentive for refueling on a biannual schedule rather than annually as has been assumed here. The major difference in the neutronic performance between

TABLE VII. Reactivity Feedback Coefficients

	Metal	Oxide
Sodium Void Reactivity, β		
Driver	3.87	2.43
IB	2.35	1.55
RB	-0.16	-0.23
AB	-	-0.17
Fuel Doppler Coefficient, $10^{-3} \text{ T } \frac{dk}{dT}$		
Flooded Doppler		
Driver	1.331	3.162
IB	1.389	3.690
RB	0.375	1.021
AB	-	0.401
Voided Doppler		
Driver	0.838	2.055
IB	0.961	2.699
RB	0.287	0.892
AB	-	0.244
Fuel Axial Expansion Coefficient, $\frac{\beta}{\text{cm}}$		
Driver	-0.783	-0.805
IB	0.0516	0.131
Radial Expansion Coefficient, $\frac{\beta}{\text{cm}}$	-1.68	-1.35
Beta-Effective	3.381×10^{-3}	3.229×10^{-3}

the two is an increase in the reactivity needed to overcome the extension of the cycle length. This cycle extension results in an increase in the reactivity swing from 1.65%Δk to 3.86%Δk for the oxide core and from 1.16%Δk to 2.63%Δk for the metal core. This increases the primary system control requirements by about 50%. To accommodate this increase in the primary control system requirement, the interchangeability constraint must be loosened and a central control rod must be placed in row 1 for the oxide core configuration. This results in a primary system of 9 rods (6 row 4 rods and 3 row 7 rods), and a secondary system which consists of 4 rods (3 row 7 rods and a central rod). The maximum rod worths, with fully enriched rods, would still fall slightly below the minimum requirements for the oxide core. In contrast, for the metal core the assignment of 9 primary rod positions (6 row 4 and 3 row 7) and 3 secondary rod positions (3 row 7), with the primary rods enriched to 25% in B-10 and the secondary rods to 50%, meets the requirements with no introduction of a new rod assembly and loss of blanket assembly.

CONCLUSIONS

In this paper we have identified and quantified those physics parameters which differentiate metal and oxide fuel types when the cores are designed to meet the constraint of interchangeability. The study shows that although small oxide and metal cores, designed to the same ground rules, exhibit many similar performance characteristics, they differ substantially in reactivity coefficients, control strategies, and fuel cycle options. It is recognized that the metallic fuel alloy considered here has not, to date, been developed to the same level of confidence as oxide fuel. However, the above results showing the greater flexibility of metal-fueled cores for meeting performance goals and safety margins in a constrained design environment provide an incentive for vigorous development of the metal fuel option.

REFERENCES

1. Y. I. CHANG, J. F. MARCHATERRE, and R. H. SEVY, "The Integral Fast Reactor Concept," Trans. Am. Nucl. Soc., 47, 293 (1984).
2. L. C. WALTERS, B. R. SEIDEL, and J. H. KITTEL, "Performance of Metallic Fuels and Blankets in Liquid-Metal Fast Breeder Reactors," Nucl. Technol., 65, 179 (1984).
3. S. F. SU and R. H. SEVY, "Inherent Accommodation of Unprotected Loss-of-Flow Accidents in LMFBRs," Trans. Am. Nucl. Soc., 47, 300 (1984).
4. L. BURRIS, M. STEINDLER, and W. MILLER, "A Proposed Pyrometallurgical Process for Rapid Recycle of Discharged Fuel Materials from the Integral Fast Reactor," Proc. Fuel Reprocessing and Waste Management Meeting, Jackson, Wyoming, August 1984.
5. L. BURRIS and L. C. WALTERS, "The Proposed Fuel Cycle for the Integral Fast Reactor," Trans. Am. Nucl. Soc., 49, 90 (1985).
6. J. E. CAHALAN, R. H. SEVY, and S. F. SU, "Accommodation of Unprotected Accidents by Inherent Safety Design Features in Metallic and Oxide-Fueled LMFBRs," Proc. Fast Reactor Safety Meeting, Knoxville, Tennessee, April 1985.

Acknowledgments

We would like to thank Dave Wade for his review of the paper.

This work was prepared under the auspices of the U.S. Department of Energy.